

# The diagnostic value of SE MRI and DWI of the spine in patients with monoclonal gammopathy of undetermined significance, smouldering myeloma and multiple myeloma

Julie C. Dutoit · Matthias A. Vanderkerken ·  
Joris Anthonissen · Frederick Dochy ·  
Koenraad L. Verstraete

Received: 18 December 2013 / Revised: 4 June 2014 / Accepted: 7 July 2014 / Published online: 9 August 2014  
© European Society of Radiology 2014

## Abstract

**Objectives** To evaluate DWI of the bone marrow in the differentiation of monoclonal gammopathy of undetermined significance (MGUS), smouldering myeloma (SMM) and multiple myeloma (MM).

**Methods** The retrospective study includes 64 patients with MGUS, 27 with SMM, 64 with new MM and 12 controls. Signal intensity (SI) of spinal SE-MRI and DWI (b0-1000) as well as apparent diffusion coefficients (ADC) were measured in the T10 and L3. Qualitative assessment of b-images was performed by one experienced radiologist.

**Results** ADC600 and ADC1000 are the best ADC values in differentiating patient groups ( $p < 0.030$ ). SIT2, SIb1000 and ADC1000 are higher and SIT1 lower in L3 compared to T10 ( $p < 0.050$ ). All quantitative parameters of L3 can differentiate significantly between MGUS and MM ( $p < 0.050$ ) and between patients with percentage plasma cells (PC%) between 0-10 % compared to >50 % ( $p = 0.001$ ). Only SIT2 for L3 can differentiate MGUS from SMM ( $p = 0.044$ ) and PC%0-10 from PC%10-25 ( $p = 0.033$ ). Qualitative interpretation of

b1000 images allows differentiating MM patients from those with MGUS or SMM ( $p < 0.001$ ).

**Conclusions** Spinal SE-MRI can differentiate among MGUS, SMM, MM and control subjects. DWI based on the SI on b1000 images and ADC values is increased in MM compared to MGUS and SMM. Qualitative assessment of b-images can differentiate MM from MGUS or SMM.

## Key points

- ADC values are higher in patients with MM compared to MGUS
- DWI parameters change late in disease evolution
- DWI is sensitive but not specific in diagnosing patients with MM
- Qualitative DWI assessment is good in detecting myeloma patients

**Keywords** Diffusion-weighted imaging · Magnetic resonance imaging · Multiple myeloma · Monoclonal gammopathy of undetermined significance · Diagnosis

J. Anthonissen  
Ghent University, De Pintelaan 185, 9000 Ghent, Belgium  
e-mail: Joris.Anthonissen@ugent.be

J. C. Dutoit (✉) · M. A. Vanderkerken · F. Dochy · K. L. Verstraete  
Department of Radiology, Ghent University Hospital, De Pintelaan  
185, 9000 Ghent, Belgium  
e-mail: julie.dutoit@ugent.be

M. A. Vanderkerken  
e-mail: Matthias.Vanderkerken@UGent.be

F. Dochy  
e-mail: Frederick.Dochy@UGent.be

K. L. Verstraete  
e-mail: Koenraad.Verstraete@UGent.be

## Abbreviations

IMWG	International Myeloma Working Group
MRI	Magnetic resonance imaging
CT	Computed tomography
PET	Positron emission tomography
DWI	Diffusion-weighted imaging
ADC	Apparent diffusion coefficient
SI	Signal intensity
MGUS	Monoclonal gammopathy of undetermined significance
SMM	Smouldering myeloma
MM	Multiple myeloma
ISS	International Staging System
HME	Hereditary multiple exostoses

NF	Neurofibromatosis
EPI	Echo planar imaging
ROI	Region of interest
T	Thoracic
L	Lumbar
ROC	Receiver-operating characteristic
AUC	Area under the curve
PC%	Percentage plasma cells
T1	T1 weighted
fsT2	Fat-suppressed T2 weighted
ST	Slice thickness
TSE	Turbo spin echo
TR	Repetition time
TE	Echo time
TI	Inversion time

## Introduction

The International Myeloma Working Group (IMWG) criteria are based on the detection of lytic lesions in mineralised bone for the diagnosis of multiple myeloma (MM). Magnetic resonance imaging (MRI) has the possibility to assess not only bone destruction, but also bone marrow infiltration and disease activity [1, 2], making this the most sensitive technique for detection of pathologies restricted to the bone marrow, even if trabecular bone is not destroyed [3]. Diffusion-weighted MR imaging (DWI), an imaging technique derived from MRI, is increasingly being used to assess bone marrow because of its sensitivity to cell density, the relative content of fat and marrow cells, water content and bone marrow perfusion [4]. The signal intensity on DWI relies on the stochastic Brownian motion, or self-diffusion, of water molecules at microscopic level within tissues [5].

Solid tumours are characterised by lower ADC values because increasing cell density limits diffusion compared to normal tissue [6, 7]. The unique structure of bone marrow causes quite paradoxical diffusion effects, because the ADC and thus water diffusivity of bone marrow invaded by tumour cells are higher than those of normal bone marrow [8–10]. The positive correlation between ADC values and cellularity in bone marrow can be explained by the distribution and characteristics of yellow and red marrow. Yellow marrow has an abundance of fat cells and reduced water content and proton density resulting in low ADC values and signal intensity (SI) on b-value images. Red marrow is characterised by a higher cellularity and lower fat content resulting in a higher water content and proton diffusivity, resulting in an increase in ADC value and SI on b-value images [4]. Nevertheless, current available data regarding pathological ADC ranges of bone marrow in patients with monoclonal gammopathy of

undetermined significance (MGUS) or MM are scarce and based on rather small patient cohorts [4, 8–14].

The objective of this study is to identify and explain the complex diffusion characteristics of vertebral bone marrow in patients with plasma cell dyscrasia and particularly its use in the diagnostic workup of patients with MGUS, SMM and MM.

## Materials and methods

### Patients

This observational retrospective study was conducted at our University Hospital and approved by the institutional ethics committee. The study population consists of 155 patients, referred by a haematologist and before receiving any kind of therapy, and 12 control subjects with a total of 167 SE MRI and DWI investigations of the spine between May 2005 and July 2013. The patients were classified according to the IMWG diagnostic criteria [15] ( $n$ =patients=investigations; mean age; sex): MGUS ( $n$ =64; 61 years; 54 % male), SMM ( $n$ =27; 63 years, 46 % male) and new MM ( $n$ =64; 61 years; 61 % male). The control subjects ( $n$ =12; 41 years; 35 % male) included investigations of patients with hereditary multiple exostoses (HME,  $n$ =4), neurofibromatosis (NF,  $n$ =6) and healthy persons ( $n$ =2). Thirteen of the 64 newly diagnosed patients presented with fractured myeloma vertebrae in the thoracic spine.

### Laboratory investigations

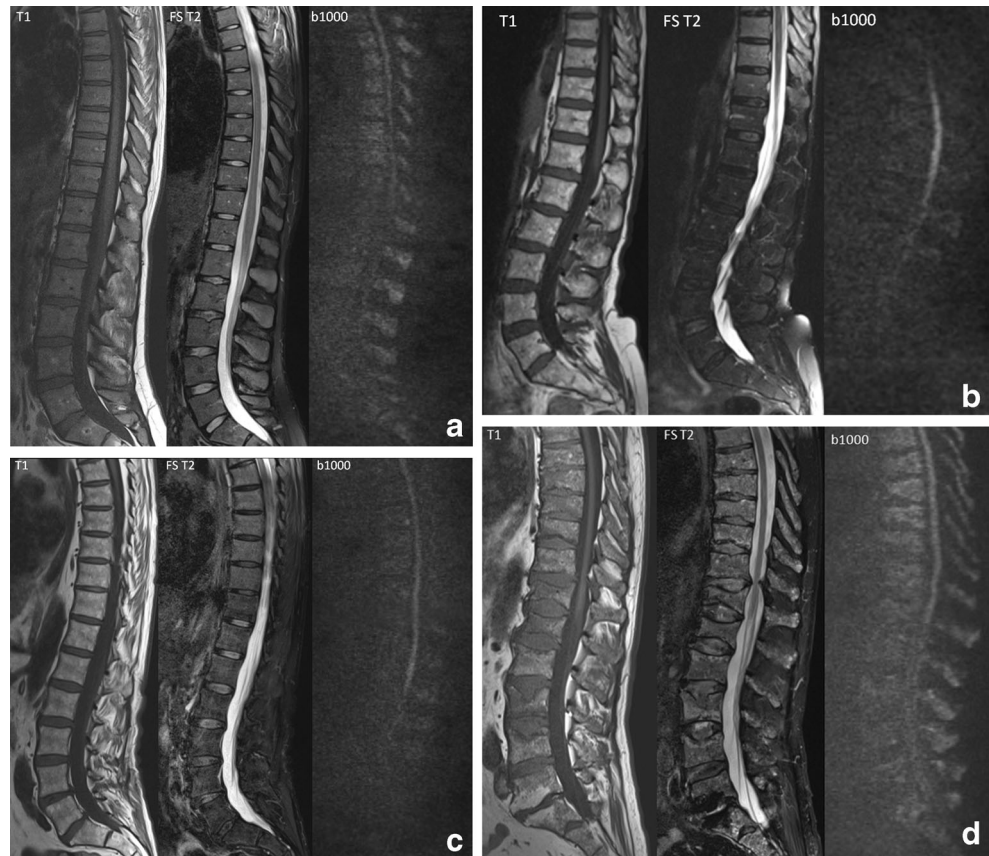
The percentage plasma cells resulting from bone marrow analysis, based on biopsy of the iliac crest, is still the gold standard for the diagnosis of MM and can therefore be used as a comparative diagnostic parameter [16, 17]. Biopsies were obtained from 135 patients, MGUS ( $n$ =47), SMM ( $n$ =26) and MM ( $n$ =62). Only the results of biopsies performed within a time range of one month before or after the MRI investigation were included.

### Imaging protocol

#### *SE MRI of the thoracolumbar spine*

Imaging was performed on a 1.5-T MRI scanner (Magnetom Avanto, Siemens Healthcare, Erlangen, Germany). Sagittal images of the spine were performed using multiple surface coils, T1-weighted (T1) TSE (TR =576 ms, TE =10 ms, ST =3 mm, matrix size =1,152×384) and fat-suppressed T2-weighted (fsT2) TSE (TR =7,270 ms, TE =68 ms, ST =3 mm, TI =140, matrix size =1,152×384) (Fig. 1).

**Fig. 1** SE MRI and diffusion-weighted imaging of the spine in patient groups based on IMWG criteria and control subjects. T1-weighted, fat-suppressed T2-weighted and b1000 images of (a) control subject and a patient with (b) monoclonal gammopathy of undetermined significance, (c) smouldering myeloma and (d) multiple myeloma



#### *Diffusion-weighted MRI of the thoracolumbar spine*

Sagittal diffusion-weighted images of the thoracolumbar spine were obtained with echo planar imaging (EPI) sequences (TR=7,700, TE=86). Before 2009, only  $b = 0$  and  $b = 1,000$  s/mm<sup>2</sup> were used. Afterwards, the DWI protocol was expanded and three other b-values were added: 200, 400 and 600 s/mm<sup>2</sup> (Fig. 1).

#### *Data analysis*

Qualitative evaluation was performed by a musculoskeletal radiologist with 25 years of experience, blinded from patient characteristics, disease stage and laboratory findings.

#### *SE imaging of the thoracolumbar spine*

The MR images were assessed quantitatively by evaluating the signal intensity of the bone marrow with the region-of-interest (ROI) method. On the sagittal T1 and fsT2 images ROIs were placed in the anterior part of thoracic vertebra T10 and lumbar vertebra L3, avoiding the basivertebral vein. The size of the ROIs was approximately 10 mm<sup>2</sup> and degenerative parts of the vertebrae as well as the intervertebral disc were avoided (Fig. 2).

#### *Diffusion-weighted MRI of the thoracolumbar spine*

Syngo MR VB17 software (Siemens Healthcare, Erlangen, Germany) was used to calculate ADC values by post-

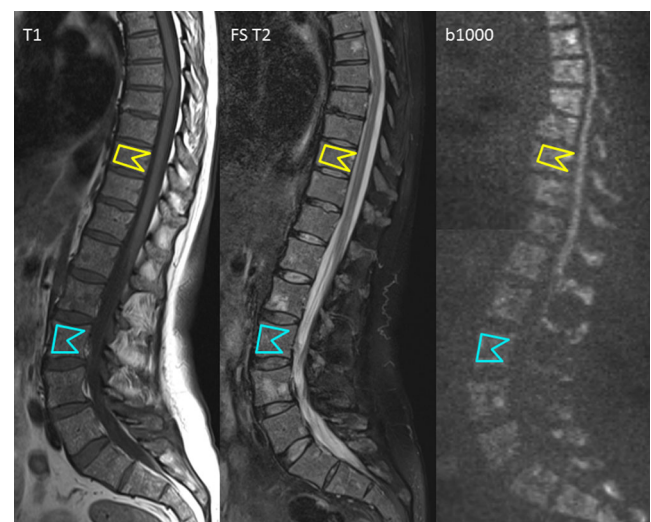


**Fig. 2** SE MRI and diffusion-weighted imaging of the spine with drawing of a region of interest (ROI) in patients with multiple myeloma. (a) T1-weighted, (b) fat-suppressed T2-weighted images and (c) b1000 images of the thoracolumbar spine with b values of 0 s/mm<sup>2</sup> and 1000 s/mm<sup>2</sup>. A region of interest (ROI) is drawn in the tenth thoracic and third lumbar vertebra, excluding the basivertebral vein

processing analysis. Six ADC maps were created, each consisting of 12 parasagittal slices, using different b-value combinations. In the first four ADC maps, the b-value 0 s/mm<sup>2</sup> was combined with b = 200 s/mm<sup>2</sup> (ADC<sub>200</sub>), b = 400 s/mm<sup>2</sup> (ADC<sub>400</sub>), b = 600 s/mm<sup>2</sup> (ADC<sub>600</sub>) and b = 1,000 s/mm<sup>2</sup> (ADC<sub>1000</sub>) respectively. A fifth map (ADC<sub>200-400-600</sub>) was created by combining 200, 400 and 600 s/mm<sup>2</sup> values. In the last ADC map (ADC<sub>0-200-400-600-1000</sub>) all five b-values were used. ROIs were drawn in the vertebral bodies of the 10th thoracic and 3rd lumbar vertebra, excluding the basivertebral vein (Fig. 2). The b1000 images were qualitatively assessed by giving a patient a ‘positive’ score when visual delineation of the vertebral bodies (diffuse) or a focal lesion (nodular) from the background noise was possible. The patient score was ‘negative’ when no difference could be seen between vertebral body and background noise [18]. We used b1000 images because a b-value of more than 800 s/mm<sup>2</sup> usually results in significant signal suppression of normal tissues or background signal intensity, allowing foci of high signal intensity with impeded diffusion to be more readily identified [19].

#### Statistics

Statistical analysis was preceded by a Shapiro-Wilk test for all quantitative parameters, demonstrating no normal distribution ( $p < 0.001$ ). Nonparametric Kruskal-Wallis tests were executed for the evaluation of differences between multiple subgroups. Post-hoc Mann-Whitney U tests after Bonferroni correction were conducted to evaluate differences between two subgroups. Paired analyses on data of the thoracolumbar spine and spinal fractures were performed using a Wilcoxon signed rank test. The optimal cutoff values for DWI parameters in diagnosing MM were determined using receiver-operating characteristic (ROC) curve analysis with the calculation of the Youden index. Results were considered to be statistically significant at  $p < 0.050$ . All statistical analyses

were performed with SPSS software (SPSS statistics version 20.0, IBM, Amonk, NY, USA).

#### Results

##### Descriptive features on SE MRI and DWI parameters for different subgroups

The mean values of signal intensity on T1, fsT2 and b1000 images and mean value of ADC<sub>1000</sub> for subgroups based on IMWG criteria (MGUS, SMM and MM) and for subgroups based on the percentage plasma cells in the bone marrow (PC%) are displayed in Tables 1 and 2, for T10 and L3 respectively.

In Table 3 detailed information on ADCs calculated from different b-value images (ADC<sub>200</sub>, ADC<sub>400</sub>, ADC<sub>600</sub>, ADC<sub>1000</sub>, ADC<sub>200-400-600</sub>, ADC<sub>0-200-400-600-1000</sub>) for T10 and L3 is summarised for subgroups based on IMWG criteria and control subjects. Data derived from subgroups based on PC% are displayed in Table 4.

##### Statistical analysis of SE MRI and DWI parameters for different subgroups

##### Comparing ADCs derived from different b-value images

Analysis of ADCs derived from different b-value images was conducted on the 86 patients who received b200, b400 and b600 images apart from the standard b0 and b1000. The ADC values were calculated and tested (Kruskal-Wallis) for their ability to differentiate among patients with MGUS, SMM, MM and control subjects (Table 3). The results derived from this statistical analysis are displayed in Table 5. Only data derived from ADC<sub>600</sub>, ADC<sub>1000</sub>, ADC<sub>200-400-600</sub> and ADC<sub>0-200-400-600-1000</sub> yielded significant results for both T10 and L3. Analysis of ADC<sub>1000</sub> with data for all patients ( $n = 167$ )

**Table 1** Mean value and standard deviation of parameters ADC<sub>1000</sub> for T10, signal intensity (SI) on b1000-images, SI on T1- and T2-weighted images for subgroups based on IMWG criteria and for subgroups based on plasma cell percentage (PC%)

Mean [SD]	ADC <sub>1000</sub> ( $\times 10^{-4}$ mm <sup>2</sup> /s)	SI b1000 (aU)	SI T1 (aU)	SI FS T2 (aU)
Control subjects	4.04 [2.74]	23.02 [7.59]	237.73 [75.37]	139.08 [71.74]
MGUS	4.32 [2.37]	20.73 [8.82]	247.93 [84.29]	90.13 [45.84]
SMM	3.78 [2.80]	20.44 [8.60]	235.33 [79.32]	123.80 [70.05]
MM	4.94 [3.07]	26.54 [8.90]	184.15 [69.47]	197.19 [147.53]
PC% 0-10	4.38 [2.37]	22.13 [9.43]	246.45 [85.25]	99.47 [59.62]
PC% 10-25	4.23 [3.44]	23.05 [7.95]	199.17 [66.34]	175.40 [162.90]
PC% 25-50	5.30 [2.92]	23.58 [7.83]	186.52 [93.12]	148.19 [90.28]
PC% >50	5.41 [2.20]	27.06 [12.70]	172.07 [40.53]	220.59 [144.28]

Abbreviations: SD standard deviation, PC% percentage plasma cells, aU arbitrary units, SI signal intensity, T1 T1 weighted, FS T2 fat suppressed T2 weighted, ADC apparent diffusion coefficient

**Table 2** Mean value and standard deviation of parameters ADC<sub>1000</sub>, measured in L3, signal intensity (SI) on b1000-images, SI on T1- and fat suppressed T2-weighted images in subgroups based on IMWG criteria and in subgroups based on plasma cell percentage (PC%)

Mean [SD]	ADC <sub>1000</sub> ( $\times 10^{-4}$ mm <sup>2</sup> /s)	SI b1000 (aU)	SI T1 (aU)	SI FS T2 (aU)
Control subjects	2.94 [1.99]	25.50 [6.03]	153.76 [67.69]	121.56 [47.46]
MGUS	2.63 [1.33]	20.29 [8.61]	237.39 [93.69]	67.36 [47.64]
SMM	2.78 [1.40]	19.88 [8.14]	237.77 [111.00]	93.24 [59.35]
MM	3.65 [2.09]	26.50 [8.95]	168.27 [71.00]	150.45 [108.55]
PC% 0-10	2.78 [1.69]	21.35 [8.74]	233.90 [98.26]	73.55 [46.81]
PC% 10-25	2.90 [1.43]	22.36 [8.02]	196.92 [81.88]	110.44 [80.75]
PC% 25-50	3.17 [1.83]	23.16 [8.57]	181.45 [93.35]	112.35 [62.25]
PC% >50	4.41 [1.98]	27.99 [11.96]	144.89 [45.11]	192.73 [140.89]

Abbreviations: *SD* standard deviation, *PC%* percentage plasma cells, *aU* arbitrary units, *SI* signal intensity, *T1* T1-weighted, *FS T2* fat suppressed T2-weighted, *ADC* apparent diffusion coefficient

yielded significant results only for L3 ( $p=0.036$ ) and not for T10 ( $p=0.246$ ).

#### Comparing signal intensities derived from different b-value images

Analysis of the SI on b-images for T10 and L3 yielded significant results for SI b0 ( $p_{T10}=0.001$ ;  $p_{L3}<0.001$ ) as well as for SI b1000 ( $p_{T10}=0.001$ ;  $p_{L3}=0.001$ ). Further analyses were based on the SI on b1000 images because statistical results for mean ADC<sub>600</sub> and ADC<sub>1000</sub> values are nearly equally significant, and because this parameter comprises a larger part of the study population ( $n=167$ ) which allows comparison with SI on b1000 images. Moreover, this parameter is better suited for evaluation of cellularity and less influenced by the T2 shine-through effect and perfusion [20].

#### Comparing data derived from T10 and L3

Analysis of the ADC<sub>1000</sub> values of T10 and L3 in all patients yielded significantly higher ADC<sub>1000</sub> values at the thoracic compared to lumbar level ( $p<0.001$ ). Moreover, the signal intensity on T1 images was significantly lower for T10 than L3 ( $p<0.001$ ), with a significantly higher signal intensity on T2-weighted images ( $p<0.001$ ) (Table 1).

#### Comparing parameters derived from conventional MRI and DWI images between subgroups

Additional statistics (Kruskall-Wallis) were performed to investigate whether parameters derived from SE MRI and DWI images, measured in T10 and L3, could significantly differentiate between patients with MGUS, SMM or MM and control subjects. This yielded significant results for all data

**Table 3** Mean ADC of the tenth thoracic and third lumbar vertebra in patients with monoclonal gammopathy of undetermined significance, smouldering myeloma and multiple myeloma

Mean ADC [SD] (n)		MGUS	SMM	New MM	Controls
ADC <sub>200</sub>	T10	8.54 [2.61] (21)	8.02 [2.77] (13)	9.72 [3.00] (42)	9.05 [1.87] (9)
	L3	8.68 [2.07] (21)	7.90 [2.03] (13)	9.60 [3.11] (42)	7.86 [1.29] (9)
ADC <sub>400</sub>	T10	4.56 [1.25] (21)	4.33 [1.13] (13)	6.21 [2.71] (42)	4.99 [1.49] (9)
	L3	4.91 [1.00] (21)	4.36 [1.00] (13)	6.05 [2.52] (42)	4.39 [1.02] (9)
ADC <sub>600</sub>	T10	5.64 [1.09] (21)	3.04 [1.15] (13)	4.99 [2.75] (42)	3.79 [1.28] (9)
	L3	3.24 [0.92] (21)	3.06 [0.68] (13)	4.67 [2.26] (42)	3.03 [0.71] (9)
ADC <sub>1000</sub>	T10	4.30 [2.35] (62)	3.79 [2.80] (26)	4.90 [3.07] (62)	4.51 [4.20] (11)
	L3	2.63 [1.33] (62)	2.78 [1.40] (26)	3.65 [2.09] (64)	2.94 [1.99] (11)
ADC <sub>200-400-600</sub>	T10	2.69 [0.92] (15)	2.70 [0.73] (13)	4.37 [2.53] (36)	3.46 [0.90] (8)
	L3	2.93 [0.66] (15)	3.08 [0.70] (13)	4.12 [1.75] (64)	3.05 [0.58] (8)
ADC <sub>0-200-400-600-1000</sub>	T10	1.87 [0.98] (15)	1.71 [0.64] (13)	3.41 [2.45] (38)	2.69 [1.26] (8)
	L3	1.77 [0.69] (15)	1.68 [0.28] (13)	3.05 [1.87] (38)	1.79 [0.68] (8)

ADC values are in  $\times 10^{-4}$  mm<sup>2</sup>/s. Note that the number of patients differs depending on the b values used (b=200, 400 or 600 s/mm<sup>2</sup> were implemented later).

*SD* standard deviation, *n* number of patients, *T10* tenth thoracic vertebra, *L3* third lumbar vertebra

**Table 4** Mean ADC of the tenth thoracic and third lumbar vertebra in patients with MGUS, SMM or MM divided into subgroups based on plasmocytosis (PC%): PC% 0-10, PC% 10-25, PC% 25-50, PC% >50 and control subjects

Mean ADC (±SD)(n)		PC% 0-10	PC% 10-25	PC% 25-50	PC% >50	Controls
ADC <sub>200</sub>	T10	8.59 [±2.63] (20)	8.80 [±2.62] (21)	10.21 [±4.19] (8)	11.11 [±2.77] (12)	9.05 [±1.87] (9)
	L3	8.11 [±1.82] (20)	8.43 [±2.20] (21)	9.00 [±5.21] (8)	11.20 [±2.87] (15)	7.86 [±1.29] (9)
ADC <sub>400</sub>	T10	4.55 [±1.52] (20)	5.26 [±2.33] (21)	6.51 [±3.18] (8)	7.53 [±2.38] (12)	4.99 [±1.49] (9)
	L3	4.59 [±0.98] (20)	4.78 [±1.58] (21)	5.89 [±3.00] (8)	7.83 [±2.46] (15)	4.39 [±1.02] (9)
ADC <sub>600</sub>	T10	5.78 [±10.31] (20)	4.10 [±2.71] (21)	4.98 [±2.43] (8)	6.14 [±2.80] (12)	3.79 [±1.28] (9)
	L3	3.07 [±0.75] (20)	3.46 [±1.28] (21)	4.28 [±2.11] (8)	6.34 [±2.49] (15)	3.03 [±0.71] (9)
ADC <sub>1000</sub>	T10	4.38 [±2.37] (58)	4.23 [±3.44] (35)	5.11 [±2.93] (17)	5.41 [±2.20] (18)	4.51 [±4.20] (11)
	L3	2.78 [±1.69] (61)	2.90 [±1.43] (35)	3.17 [±1.83] (17)	4.41 [±1.98] (21)	2.94 [±1.99] (11)
ADC <sub>200-400-600</sub>	T10	2.96 [±1.08] (15)	3.74 [±2.76] (20)	4.00 [±1.51] (6)	5.14 [±2.56] (11)	3.46 [±0.90] (8)
	L3	3.01 [±0.67] (18)	3.37 [±1.00] (20)	3.41 [±0.67] (6)	5.42 [±2.11] (14)	3.05 [±0.58] (8)
ADC <sub>0-200-400-600-1000</sub>	T10	2.11 [±1.09] (15)	2.76 [±2.55] (20)	2.86 [±2.10] (6)	4.41 [±2.28] (11)	2.69 [±1.26] (8)
	L3	1.86 [±0.66] (18)	2.08 [±1.06] (20)	2.73 [±1.60] (6)	4.35 [±2.14] (14)	1.79 [±0.68] (8)

ADC values are in  $\times 10^{-4}$  mm<sup>2</sup>/s. Note that the number of patients differs depending on the b values used (b=200, 400 or 600 s/mm<sup>2</sup> were implemented later) SD standard deviation, n number of patients, T10 tenth thoracic vertebra, L3 third lumbar vertebra, PC% plasmocytosis

derived from L3 ( $p < 0.050$ ) and all but the mean ADC1000 for T10 ( $p = 0.246$ ). The same analysis was done for subgroups based on the percentage plasma cells in the bone marrow. This yielded no significant results for data derived from ADC1000 ( $p = 0.098$ ) and SI on b1000 ( $p = 0.337$ ) images measured in T10 and SI b1000 measured in L3 ( $p = 0.165$ ).

Post-hoc Mann-Witney-U tests were conducted after Bonferroni correction (IMWG subgroups  $n = 4$  and  $\alpha' = 0.013$ ; PC% subgroups  $n = 5$  and  $\alpha' = 0.010$ ) on all parameters providing significant results for differentiation between subgroups and control subjects; therefore, insignificant variables of ADC<sub>1000</sub> T10 (IMWG) and of ADC<sub>1000</sub> T10, SI b1000 T10 and SI b1000 L3 (PC%) were excluded from further analysis. Results are displayed in Table 6 for subgroups based on IMWG criteria and in Table 7 for subgroups based on percentage plasma cells in the bone marrow. These tables summarise the  $p$ -values for comparing data derived from parameters ADC1000, SI on b1000 images and SI on T1 and fsT2 images for different subgroups. Combining these data with

**Table 5** ADC values derived from different b-value images ranging from 0-1000 for thoracic (T) and lumbar (L) vertebra T10 and L3, tested on their ability to differentiate between patients with MGUS, SMM, MM and control subjects (Kruskal-Wallis analysis)

p-value	T10	L3
ADC <sub>200</sub>	0.245	0.066
ADC <sub>400</sub>	0.009*	0.068
ADC <sub>600</sub>	0.020*	0.003*
ADC <sub>1000</sub>	0.028*	0.006*
ADC <sub>200-400-600</sub>	0.005*	0.013*
ADC <sub>0-200-400-600-1000</sub>	0.002*	0.009*

\* $p$  value below significance level  $\alpha$  (0.050)

**Table 6** This table represents the  $p$ -values for the signal intensity on b1000, T1-weighted and fat-suppressed T2-weighted images and for the value of ADC1000, all measured in T10 and L3; mutually comparing patients with monoclonal gammopathy of undetermined significance (MGUS), smouldering myeloma (SMM), multiple myeloma (MM) and control subjects

P value	Control subjects	MGUS	SMM	MM
T10				
P value L3	Control subjects	[a] - [b] 0.056 [c] 0.018° [d] 0.003*	[a] - [b] 0.097 [c] 0.147 [d] 0.258	[a] - [b] 0.925 [c] 0.559 [d] 0.901
	MGUS	[a] 0.909 [b] 0.053° [c] 0.004* [d] 0.001*	[a] - [b] 0.864 [c] 0.508 [d] 0.030°	[a] - [b] 0.000* [c] 0.000* [d] 0.000*
	SMM	[a] 0.715 [b] 0.070 [c] 0.024° [d] 0.117	[a] 0.725 [b] 0.774 [c] 0.872 [d] 0.044°	[a] - [b] 0.011* [c] 0.005* [d] 0.038°
	MM	[a] 0.146 [b] 0.727 [c] 0.538 [d] 0.817	[a] 0.007* [b] 0.001* [c] 0.000* [d] 0.000*	[a] 0.057 [b] 0.003* [c] 0.007* [d] 0.026°

[a] ADC1000 ( $\times 10^{-4}$  mm<sup>2</sup>/s), [b] SI b1000 (aU), [c] SI T1 (aU), [d] SIFS T2 (aU)

-=not performed because  $p > 0.050$  with Kruskal-Wallis test for all subgroups

\*= $p$  value below significance level  $\alpha'$  (0.013) after Bonferroni correction

°= $p$  value below significance level  $\alpha$  (0.050) without Bonferroni correction

**Table 7** This table represents the p-values for the signal intensity on b1000, T1-weighted and fat-suppressed T2-weighted images and for the value of ADC1000, all measured in T10 and L3, mutually comparing

subgroups based on percentage plasma cells (PC%), PC% 0-10, PC% 10-25, PC% 25-50, PC% >50 and to control subjects

P value	Control subjects	PC% 0-10	PC% 10-25	PC% 25-50	PC% >50
T10					
P value					
L3					
Control subjects		[a] - [b] - [c] 0.030° [d] 0.011°	[a] - [b] - [c] 0.717 [d] 0.571	[a] - [b] - [c] 0.352 [d] 0.616	[a] - [b] - [c] 0.487 [d] 0.603
PC% 0-10	[a] 0.847 [b] - [c] 0.012° [d] 0.004*		[a] - [b] - [c] 0.016° [d] 0.004*	[a] - [b] - [c] 0.017° [d] 0.049°	[a] - [b] - [c] 0.000* [d] 0.000*
PC% 10-25	[a] 0.558 [b] - [c] 0.101 [d] 0.301	[a] 0.642 [b] - [c] 0.099 [d] 0.033°		[a] - [b] - [c] 0.262 [d] 0.895	[a] - [b] - [c] 0.131 [d] 0.128
PC% 25-50	[a] 0.423 [b] - [c] 0.661 [d] 0.443	[a] 0.386 [b] - [c] 0.033° [d] 0.010°	[a] 0.490 [b] - [c] 0.328 [d] 0.692		[a] - [b] - [c] 0.590 [d] 0.141
PC% >50	[a] 0.036° [b] - [c] 0.921 [d] 0.309	[a] 0.001* [b] - [c] 0.000* [d] 0.000*	[a] 0.004* [b] - [c] 0.019° [d] 0.025°	[a] 0.070 [b] - [c] 0.266 [d] 0.156	

[a] ADC1000 ( $\times 10^{-4}$  mm<sup>2</sup>/s), [b] SI b1000 (a.U.), [c] SI T1 (aU), [d] SI FS T2 (aU)

-=not performed because  $p > 0.050$  with Kruskal-Wallis test for all subgroups

\*= $p$  value below significance level  $\alpha'$  (0.010) after Bonferroni correction

°= $p$  value below significance level  $\alpha$  (0.050) without Bonferroni correction

information from the descriptive statistics (Tables 1 and 2) yields more information and better understanding, e.g. SI on b1000 images for T10 ( $p < 0.001$ ) and L3 ( $p = 0.003$ ) is significantly higher in patients with MM [T10 26.54 arbitrary units (aU); L3 26.50 aU] compared to patients with MGUS (T10 20.44 aU; L3 20.29 aU).

#### Analysis of data of newly diagnosed MM patients with spinal fractures

A subgroup analysis was conducted on 13 newly diagnosed patients with MM who had pathological fractures in the thoracic spine (T9,  $n = 6$ ; T11,  $n = 2$ ; T12,  $n = 5$ ). Mean ADC<sub>1000</sub> of T10 ( $p = 0.008$ ; mean ADC<sub>1000</sub> =  $4.94 \pm 3.03 \times 10^{-4}$  mm<sup>2</sup>/s) and L3 ( $p = 0.001$ ; mean ADC<sub>1000</sub> =  $4.17 \pm 2.40 \times 10^{-4}$  mm<sup>2</sup>/s) were significantly lower compared to vertebral fractures (mean ADC<sub>1000</sub> =  $8.54 \pm 2.89 \times 10^{-4}$  mm<sup>2</sup>/s). Above, there was a significantly higher SI on b1000 images when comparing L3 ( $p = 0.012$ ; mean SI b1000 =  $12.30 \pm 6.82$  aU) with the fractured vertebra (mean SI b1000 =  $13.80 \pm 8.15$  aU), but no

difference was observed for T10 ( $p = 0.099$ ; mean SI b1000 =  $10.40 \pm 9.5$  aU). Six patients had a vertebral fracture due to a focal osteolytic lesion, and seven patients had a vertebral fracture based on osteoporotic changes due to trabecular destruction caused by a diffuse invasion pattern with a visualisation of a compression line adjacent to the vertebral endplate.

#### Value of quantitative and qualitative analysis of MRI and DWI parameters in diagnosing patients with MM from MGUS and SMM

A ROC curve was constructed for all of the above-discussed parameters for L3: SI on T1 images, SI on fsT2 images, ADC<sub>1000</sub>, SI on b1000 images and the radiological interpretation of the SI on b1000 images, as described in Materials and Methods (Fig. 3). The latter had the best area under the curve (AUC = 0.77;  $p < 0.001$ ) for differentiating MM patients from patients with MGUS or SMM, followed by the SI on fsT2 images (AUC = 0.763;  $p < 0.001$ ), performing better than the SI

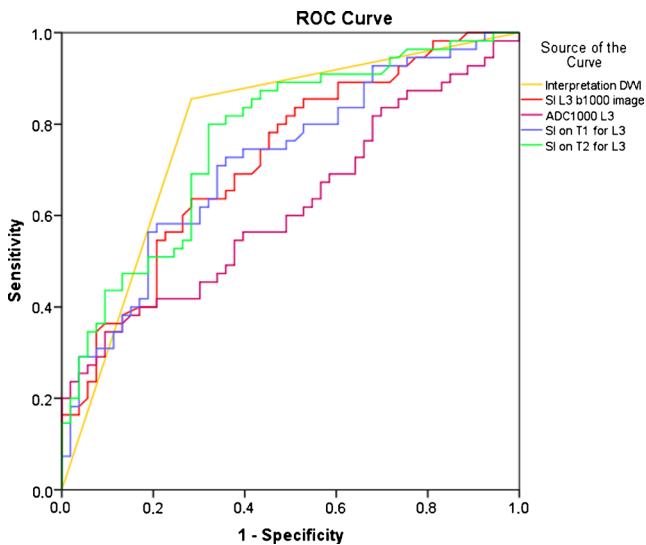


**Fig. 3** ROC curve evaluating the diagnostic accuracy of DWI parameters. Diagnostic accuracy was assessed for quantitative parameters  $ADC_{1000}$  and signal intensity on b1000, T1-weighted and fat-suppressed T2-weighted images. The fifth parameter is the qualitative interpretation of b1000 images; patients with hyperintense focal lesions or diffuse hyperintense signal intensity in the vertebral body are given a positive score on visual analysis

on T1 images ( $AUC=0.719$ ;  $p<0.001$ ). The  $ADC_{1000}$  seemed to have the weakest diagnostic performance for MM ( $AUC=0.600$ ;  $p=0.052$ ) compared to the other parameters. Patients with a positive score on radiological interpretation were characterised by a significantly higher  $ADC_{1000}$  value ( $p=0.003$ ) and SI on b1000 images ( $p<0.001$ ). The cutoff value for  $ADC_{1000}$  in diagnosing patients with MM from patients with MGUS or SMM is  $1.93 \times 10^{-4} \text{ mm}^2/\text{s}$  (sensitivity 75 %, specificity 33 %) and for SI on b1000 images 16.75 aU (sensitivity 86 %, specificity 51 %).

## Discussion

Multiple myeloma (MM) is a haematological malignancy characterised by proliferation and accumulation of monoclonal plasma cells in the bone marrow. The disease evolves from an asymptomatic stage MGUS, which progresses over SMM to symptomatic disease (MM) [16, 21]. The thoracolumbar spine and pelvic girdle are the main sites for monoclonal plasma cell infiltration [22]. SE MRI is the most sensitive technique in detecting pathologies restricted to the bone marrow [3]. However, sometimes normal red marrow has similar imaging characteristics, limiting the specificity of analyses [5]. DWI has therefore been introduced as an additional MRI application to further characterise bone marrow pathology [23] displaying cell density, water content and random motion of water molecules with ADC as a quantitative parameter for diffusivity [4]. However, current available data

regarding pathological ADC ranges of bone marrow in patients with MGUS or MM are scarce and based on rather small patient cohorts [4, 8–14]. To our knowledge, this study is the first to compare SI on SE MRI with SI and ADC derived from DWI images in these patients.

### ADCs derived from different b-value images

In general, there is a variability of reported ADCs and pulse sequences used, reducing the comparability of different studies [8]. Our analysis was based on ADCs derived from a range of b-values (Tables 3 and 4), yielding more significant results for ADCs based on b600 (T10,  $p=0.020$ ; L3,  $p=0.030$ ) and b1000 (T10,  $p=0.028$ ; L3,  $p=0.006$ ) images as compared to lower b-value images. This can be explained by the influence of T2 relaxivity and perfusion on lower b-values. Since we wanted to investigate cellularity in MM, ADCs and SIs of higher b-values were more suited for this analysis [20]. B-value images departing from 600  $\text{mm}^2/\text{s}$  seem sufficient in evaluating MM and precursor states with the EPI fat suppression technique. Messiou et al. already proposed 1,264  $\text{mm}^2/\text{s}$  as the optimum b-value when using the spectral adiabatic inversion recovery (SPAIR) fat suppression technique [12].

### Comparing data derived from T10 and L3

A thoracolumbar gradient was found demonstrating a significantly higher water content and water diffusivity at the thoracic compared to the lumbar spine (higher mean  $ADC_{1000}$  value and SI on b1000 images) in MM, MGUS and SMM (Tables 1 and 2). Hillengass et al. also found a significant decrease in ADC from the first to the fifth lumbar vertebra [14]. The lumbar bone marrow is characterised by a lower amount of red marrow and increased adipogenesis due to pronounced mechanical stress and local ischaemia [14, 24]. This was also demonstrated in our study by significantly lower SI on T1 images (lower fat content) for T10 together with a higher SI on fsT2 images (higher water content). Since it is more practical for clinical use to choose only one vertebra for functional analysis of the spine in patients with MM, L3 would be a better choice than T10. Because of the higher amount of yellow marrow at the lumbar level, more changes in ADCs occur when fat cells are replaced by plasma cells, thereby more clearly denoting plasma cell infiltration. This was confirmed in further statistical analysis, yielding more significant results for variables of SI T1, SI fsT2 and  $ADC_{1000}$  derived from L3 compared to T10 ( $p<0.001$ ). Diffusion restriction measurements in multiple myeloma are significantly better in lumbar vertebra (L3) compared to thoracic (T10).



### Characteristics of MGUS versus MM on SE MRI and DWI

We tried to assess the differences in water content and water proton diffusivity in patients with MGUS, SMM and MM based on the distribution and characteristics of yellow, red and myeloma infiltrated bone marrow by comparing data derived from SE MRI with data from DWI. A higher restriction of water diffusion was found in patients with MGUS (mean  $ADC_{1000}=2.63 \times 10^{-4} \text{ mm}^2/\text{s}$ ) compared to patients with MM (mean  $ADC_{1000}=3.65 \times 10^{-4} \text{ mm}^2/\text{s}$ ) ( $p=0.001$ ) based on the mean ADC value of L3. These mean values are comparable to the also significantly differing values found by Hillengass et al. based on pelvic crest infiltration on DWI (MGUS: mean  $ADC_{750} 2.50 \times 10^{-4} \text{ mm}^2/\text{s}$  and MM mean  $ADC_{750} 4.00 \times 10^{-4} \text{ mm}^2/\text{s}$ ) and correlating with the pelvic crest plasma cell percentage [13]. As our DWI results of the lumbar spine are in concordance with those of Hillengass et al. in the pelvis, DWI of the spine can be considered a good parameter reflecting the PC% in iliac crest biopsies.

The significant difference in  $ADC_{1000}$  between MGUS and MM can be explained by a higher bone marrow fat content in patients with MGUS (29 % higher SI on T1 images;  $p<0.001$ ) together with a lower water content (123 % lower SI on fsT2 images;  $p<0.001$ ) resulting in impeded water movement by fat cells and low SI on b1000 images ( $p=0.007$ ) because of the fat suppression pulse that is applied with the EPI diffusion-weighted measurement [25]. Yellow marrow contains mainly fat (95 % fat cells) and a small proportion of water [22, 26]. The abundance of fat cells with increased extracellular tortuosity, a hydrophobic nature and lower water proton density of yellow marrow explains the low SI and ADC value that is seen in older people and thus in patients with MGUS (mean age 61 years and a plasma cell percentage <10 %) [4, 9]. Vice versa, in MM the fat content decreases with increasing water content, resulting in higher water proton diffusivity and higher  $ADC_{1000}$  and SI on b1000.

### Characteristics of SMM on SE MRI and DWI

No differences in the  $ADC_{1000}$  value or in SI on b1000 images ( $p>0.050$ ) could be found between patients with MGUS and SMM. The fat content in their lumbar vertebra is nearly the same based on the SI on T1 images. There is only a slightly higher concentration of water in patients with SMM (SI on fsT2; T10,  $p=0.030>\alpha'$ ; L3,  $p=0.040>\alpha'$ ), indicating a starting infiltration of plasma cells (definition SMM >10 % plasma cells) with restricted diffusion and low SI on b1000 images due to the high fat content. In the evolution from patients with SMM to MM, significant increases in SI on b1000 (T10,  $p=0.011$ ; L3,  $p=0.003$ ) and fsT2 (T10,  $p=0.038>\alpha'$ ; L3,  $p=0.026>\alpha'$ ) and decreases in SI on T1 (T10,  $p=0.005$ ; L3,  $p=0.007$ ) images can be

seen, representing a higher water content and a decrease in fat content.

### Influence of percentage of plasma cells on imaging findings on SE MRI and DWI

For a better understanding of the above-described changes, we classified the population of patients with MGUS, SMM and MM into groups based on the percentage of plasma cells in the bone marrow (PC%): PC% 0-10 and PC% 10-25, PC% 25-50 and PC% >50. The SI on fsT2 increases starting from a PC% 0-10 and continues to increase until PC% >50 % (Table 7). For SI on T1 there is only a slight nonsignificant decrease with increasing plasma cell infiltration from 0 to 50 %. A significant decrease in SI on T1 and thus fat content occurs late in the evolution, in patients from the group PC% >50 %, compared to PC% 0-10 (T10 and L 3,  $p<0.001$ ). We could demonstrate that the SI on fsT2 images is an early parameter for depicting an increase in water content and increasing plasma cell infiltration, whilst at the same time there is only a slight, nonsignificant decrease in fat content, associated with a slightly higher signal intensity on T1 images and diffusion restriction by fat cells with low mean  $ADC_{1000}$  and low SI on b1000 images. The SI on T1 images, SI on b1000 images and  $ADC_{1000}$  value are rather late changing parameters: the infiltration has to be high enough to result in a decrease in fat cells and lower signal on T1 images and less diffusion restriction. This decrease in fat cells and increasing volume of intra-(plasma cells) and extracellular water are associated with a higher mean  $ADC_{1000}$  value and a high SI on b1000 images.

### Characteristics of MM versus control subjects on SE MRI and DWI

Comparison of the SI between patients with MM and control subjects yielded no significant difference in SI on b1000 images or on T1- and T2-weighted images ( $p>0.050$ ). Previous studies described higher ADC and SI values for tumoral lesions (Hillengass et al.,  $ADC_{750} 4.00 \times 10^{-4} \text{ mm}^2/\text{s}$ ) compared to normal red and yellow lumbar bone marrow (Hilengass et al.,  $ADC_{750} 2.70 \times 10^{-4} \text{ mm}^2/\text{s}$ ) [4, 13]. In our study, young control subjects (L3  $ADC_{1000} 2.94 \times 10^{-4} \text{ mm}^2/\text{s}$ ) can be differentiated from MM patients with >50 % PC (L3  $ADC_{1000} 4.41 \times 10^{-4} \text{ mm}^2/\text{s}$ ) ( $p=0.036$ ) based on ADC values, with comparable values as in previous studies [13], but not based on the SI on SE MRI and DWI images.

The control subjects in this study were mainly young people (mean age 40 years), characterised by a higher amount of red bone marrow compared to older patients with MGUS (mean age 61 years), SMM (mean age 63 years) and MM (mean age 61 years). Young bone marrow mainly consists of red bone marrow, containing less fat (40 %) and more water (40 %) with a higher cellularity (haematopoietic cells)

compared to yellow fatty (95 %) marrow [22, 26], resulting in a water content and water proton diffusivity comparable to that of myeloma infiltrated bone marrow. Padhani et al. already mentioned that differences between red marrow and myeloma are more likely to be related to an absence of fat cells and increased cellularity with higher interstitial water content and water proton density [4]. In patients with an excessive tumoral infiltration (plasmocytosis > 50 %) there are almost no fat cells left in the marrow. Although monoclonal plasma cell infiltration will cause significant changes in water content and proton diffusivity, no differences in ADC and SI between control subjects and new MM patients could be detected. This is due to the heterogeneous degree of plasma cell infiltration (10 – 100 %) in the bone marrow of the newly diagnosed MM patients causing similar changes in SI b1000 as in young control subjects. SE MRI based on SI T1 and fsT2 images also did not show differences between normal marrow and highly infiltrated marrow ( $p > 0.005$ ). In clinical practice, the mean age of patients is around 65 years, making differentiation with healthy subjects of this age less difficult because of their high amount of yellow bone marrow, as previously described for patients with MGUS. However, sometimes younger patients are affected, making the differentiation between invaded myeloma and normal red bone marrow more difficult. This problem can also be encountered in older patients receiving bone marrow-stimulating factors used in association with chemotherapy leading to red bone marrow hyperplasia [27].

### Spinal fractures

Narquin et al. described that the positive relationship between ADC values and the cellularity of the bone marrow is on the one hand clearly related to the overall water content and on the other hand also to structural tortuosity caused by fat cells and trabeculae [28]. If the content of trabeculae and fat is lower and overall water content is high, then water motion in the bone marrow occurs more actively because of less extracellular tortuosity. These findings have been confirmed by our analysis of vertebral fractures. A spinal fracture results in bone marrow oedema and disruption of trabeculae and microstructures causing an increased diffusion [5], higher ADC<sub>1000</sub> (T10,  $p = 0.008$ ; L3,  $p = 0.008$ ) and SI b1000 (T10,  $p > 0.050$ ; L3,  $p = 0.012$ ). Our results on diffusivity in malignant spinal fractures (our study,  $ADC_{1000} = 8.54 \times 10^{-4} \text{ mm}^2/\text{s}$ ) are in concordance with the data published by Dietrich et al. ( $ADC = 7.10 \times 10^{-4} \text{ mm}^2/\text{s}$ ) [8]. Moreover, we demonstrated that malignant fractured vertebra have an even higher diffusivity compared to infiltrated bone marrow in non-fractured vertebra. This is due to the low extracellular tortuosity and vast interstitium (disruption microstructures) with a high water proton density (plasma cell infiltration and oedema) and low fat content (plasma cell infiltration).

### Value of SE MRI and DWI parameters in differentiating patients with MM from MGUS and SMM

Visual assessment can provide an alternative solution to difficult calculations and quantitative assessment, and it is clinically useful, particularly in the global assessment of disseminated tumour burden. Disease progression will result in new areas of abnormal signal intensity or changes in the extent and signal intensities of abnormalities [5]. DWI is best suited for visual radiological interpretation because diffuse or focal lesions present as light grey or white on b1000 images against a dark background, making lesions readily visible for qualitative interpretation (AUC = 0.770). Although SI fsT2 has a similar AUC (0.763) in this analysis, these images alone are not sufficient because changes in SI on fsT2 are not easily visible and can only be detected by quantitative measurement of SI, which is time consuming and less practical compared to the quick qualitative visual assessment based on b1000 images. Analysis of the quantitative DWI parameters already demonstrated that the higher SI on b1000 images in MM patients (SI = 27 aU) allows good differentiation from patients with MGUS (SI = 20 aU). The cutoff value for  $ADC_{1000}$  in our study was  $1.93 \times 10^{-4} \text{ mm}^2/\text{s}$ , which is lower than those of  $ADC_{800/900}$   $7.74 \times 10^{-4} \text{ mm}^2/\text{s}$  or  $ADC_{\text{multiple b-values}}$   $6.55 \times 10^{-4} \text{ mm}^2/\text{s}$ , respectively, described by Padhani et al. and Messiou et al. [9, 29] in previous reports. An explanation could be the smaller study population and the different methods of fat suppression used: Messiou et al. used spectral selection attenuated recovery (SPAIR) ( $n = 20$  patients); we used the same inversion recovery fat suppression technique like Padhani et al. ( $n = 49$  patients) [29]. The difference between our results and those of Padhani et al. can be explained by the heterogeneous population in their analysis: metastasis and myeloma were pooled as ‘malignant bone marrow’, in contrast to our homogeneous patient group with plasma cell dyscrasias. Their control population with ‘normal marrow’ consisted of patients with metastatic disease in remission (red or yellow marrow) or receiving chemotherapy with growth colony-stimulating factor (red marrow), and moreover they compared ROIs provided information on different body bone marrow locations [29]. Actual comparison of the different cutoff values of our more homogeneous group of patients with their heterogeneous population is thus not possible. Our calculated optimal cutoff values for  $ADC_{1000}$  ( $1.93 \times 10^{-4} \text{ mm}^2/\text{s}$ ) and SI on b1000 images (16,75 aU) are not clinically useful because the value is lower than the observed mean values for SMM and MGUS and the sensitivity (ADC 75 %, SI 86 %) is moderate with a very low specificity (ADC 33 %, SI 51 %).

## Value of qualitative interpretation of b1000 images

We qualitatively evaluated the b1000-images looking for diffuse SI increases of the entire vertebra and for focal lesions, compared to background noise, without knowledge of ADC<sub>1000</sub> values. This radiological interpretation seemed the best DWI parameter in differentiating patients with MM from patients with MGUS or SMM (AUC=0.77;  $p<0.001$ ), reflecting their lower fat content and higher water proton diffusivity (Fig. 3). This confirms the findings of Narquin et al. that only visual analysis is sufficient for differentiating patients with MM [18]. The qualitative evaluation correlated significantly with our quantitative parameters; patients with a positive score had higher ADC<sub>1000</sub> values ( $p=0.003$ ) and SI on b1000 images ( $p<0.001$ ). However, the value of the calculation of ADC seemed limited in differentiating MM from MGUS ( $p=0.052$ ). Narquin et al. first stated that only visual analysis of DWI images seemed sufficient since the ADC values cannot be reproduced from one machine to another, vary in the same patient by at least 14 % in time and render a more complex reading [18]. As demonstrated above, this visual evaluation method is mainly useful in clear-cut cases, especially in diagnosing patients with a plasma cell percentage of more than 50 %. Moreover, patients with a positive visual radiological evaluation are characterised by a lower survival and thus worse prognosis. Problems will arise for the evaluation of MM patients with a lower percentage of plasma cell infiltration and thus a higher amount of fat cells in the bone marrow, causing a lower signal intensity on b1000 images. Combined visual evaluation of SI on fsT2 images as an early parameter might be useful in those cases (Table 7): PC% 0-10 vs. PC% 10-25 ( $p=0.033>\alpha'$ ), PC% 10-25 vs. PC% 25-50 ( $p=0.033>\alpha'$ ) and PC% 25-50 vs. PC% >50 ( $p<0.001$ ).

However, a number of pitfalls have to be taken into account when visually analysing high b-value images, related to the fact that DW images reflect both cellular as well as the water content of tissues. Tissue oedema secondary to fracture and degenerative disease can present with high signal intensity on b-value images, i.e. the 'T2-shine-through' effect. It is essential to correlate findings on b-value images with ADC maps and especially with analysis of morphological appearances on SE MRI to avoid misinterpretations arising from visual assessment of signal intensity [5].

## Limitations

A limitation of this study is the observational retrospective design. Patients included before 2009 only received b0 and

b1000 images. In this study the images were analysed by one experienced musculoskeletal radiologist, because the interpretation of 1900 anatomical and functional images was very time consuming. Since the observer was blinded from patient information and the mean time between two MRI investigations is 1 year, there was no risk of recall bias. Another limitation is the post-processing technique with the region-of-interest method, which is operator dependent and sensitive to variation between acquisition protocols. We did not perform intravoxel incoherent motion (IVIM) analysis to determine or exclude the influence of microcirculation on diffusion results. Since the analysis mainly focuses on high b-values (b1000), this influence is negligible and pure diffusion characteristics are approached [1, 19]. A potential source of error of the DWI protocol used in the present study may be residual fat signal after fat suppression. This may be further investigated using fat diffusion [1].

## Conclusion

In a preselected population by haematological analysis SE MRI based on the evaluation of SI on fat-suppressed T2-weighted images can differentiate patients with MGUS, SMM, MM and control subjects and correlates with the plasma cell increase in the bone marrow. The SI on T1-weighted images is a rather late-changing parameter and is able to differentiate MM from MGUS and SMM. This parameter decreases significantly when there is a plasma cell infiltration of more than 50 %. The SI on b1000 images and the related ADC values on which diffusion-weighted imaging is based are increased in patients with MM compared to MGUS and SMM, especially in patients with a high plasma cell percentage, resulting in higher water proton diffusivity. Qualitative interpretation of lesion activity by visually assessing DWI images is the best parameter for differentiating patients with MM from patients with MGUS and SMM. However, biopsies remain important for pre-selection of patients, especially for the distinction between myeloma marrow and red bone marrow.

**Acknowledgments** The scientific guarantor of this publication is Koenraad Verstraete. The authors of this manuscript declare no relationships with any companies, whose products or services may be related to the subject matter of the article. The authors state that this work has not received any funding. One of the authors has significant statistical expertise. Institutional Review Board approval was obtained. Written informed consent was waived by the Institutional Review Board. Some study subjects or cohorts have been previously reported in Euro J Radiol. A correlation was made between data of conventional whole-body MRI and dynamic contrast-enhanced MRI. Methodology: retrospective, diagnostic or prognostic study/observational, performed at one institution.

## References

- Shah R, Stieltjes B, Andrulis M et al (2013) Intravoxel incoherent motion imaging for assessment of bone marrow infiltration of monoclonal plasma cell diseases. *Ann Hematol* 92:1553–1557
- Dutoit JC, Vanderkerken MA, Verstraete KL (2013) Value of whole body MRI and dynamic contrast enhanced MRI in the diagnosis, follow-up and evaluation of disease activity and extent in multiple myeloma. *Eur J Radiol* 82:1444–1452
- Schmidt GP, Reiser MF, Baur-Melnyk A (2007) Whole-body imaging of the musculoskeletal system: the value of MR imaging. *Skelet Radiol* 36:1109–1119
- Padhani AR, van Ree K, Collins DJ, D'Sa S, Makris A (2013) Assessing the relation between bone marrow signal intensity and apparent diffusion coefficient in diffusion-weighted MRI. *AJR Am J Roentgenol* 200:163–170
- Khoo MM, Tyler PA, Saifuddin A, Padhani AR (2011) Diffusion-weighted imaging (DWI) in musculoskeletal MRI: a critical review. *Skelet Radiol* 40:665–681
- Petralia G, Thoeny HC (2010) DW-MRI of the urogenital tract: applications in oncology. *Cancer Imaging* 10 Spec no A:S112–S123
- Kitajima K, Takahashi S, Ueno Y et al (2013) Do apparent diffusion coefficient (ADC) values obtained using high b-values with a 3-T MRI correlate better than a transrectal ultrasound (TRUS)-guided biopsy with true Gleason scores obtained from radical prostatectomy specimens for patients with prostate cancer? *Eur J Radiol* 82:1219–1226
- Dietrich O, Biffar A, Reiser MF, Baur-Melnyk A (2009) Diffusion-weighted imaging of bone marrow. *Semin Musculoskelet Radiol* 13:134–144
- Messiou C, Collins DJ, Morgan VA, Desouza NM (2011) Optimising diffusion weighted MRI for imaging metastatic and myeloma bone disease and assessing reproducibility. *Eur Radiol* 21:1713–1718
- Padhani AR, Koh DM, Collins DJ (2011) Whole-body diffusion-weighted MR imaging in cancer: current status and research directions. *Radiology* 261:700–718
- Fenchel M, Konaktchieva M, Weisel K et al (2010) Early response assessment in patients with multiple myeloma during anti-angiogenic therapy using arterial spin labelling: first clinical results. *Eur Radiol* 20:2899–2906
- Messiou C, Giles S, Collins DJ et al (2012) Assessing response of myeloma bone disease with diffusion-weighted MRI. *Br J Radiol* 85:e1198–e1203
- Hillengass J, Bauerle T, Bartl R et al (2011) Diffusion-weighted imaging for non-invasive and quantitative monitoring of bone marrow infiltration in patients with monoclonal plasma cell disease: a comparative study with histology. *Br J Haematol* 153:721–728
- Hillengass J, Stieltjes B, Bauerle T et al (2011) Dynamic contrast-enhanced magnetic resonance imaging (DCE-MRI) and diffusion-weighted imaging of bone marrow in healthy individuals. *Acta Radiol* 52:324–330
- International Myeloma Working G (2003) Criteria for the classification of monoclonal gammopathies, multiple myeloma and related disorders: a report of the International Myeloma Working Group. *Br J Haematol* 121:749–757
- Landgren O, Korde N (2011) Multiple myeloma precursor disease: current clinical and epidemiological insights and future opportunities. *Oncology (Williston Park)* 25:589–590
- Landgren O, Waxman AJ (2010) Multiple myeloma precursor disease. *Jama* 304:2397–2404
- Narquin S, Ingrand P, Azais I et al (2013) Comparison of whole-body diffusion MRI and conventional radiological assessment in the staging of myeloma. *Diagn Interv Imaging* 94:629–636
- Koh DM (2010) Qualitative and quantitative analyses: image evaluation and interpretation. In: Koh DM, Thoeny HC (eds) *Diffusion-weighted MR imaging applications in the body*. Springer, Heidelberg, pp 33–47
- Padhani AR, Khan AA (2010) Diffusion-weighted (DW) and dynamic contrast-enhanced (DCE) magnetic resonance imaging (MRI) for monitoring anticancer therapy. *Target Oncol* 5:39–52
- Landgren O (2010) Monoclonal gammopathy of undetermined significance and smoldering myeloma: new insights into pathophysiology and epidemiology. *Hematol Am Soc Hematol Educ Program* 2010:295–302
- Silva JR Jr, Hayashi D, Yonenaga T et al (2013) MRI of bone marrow abnormalities in hematological malignancies. *Diagn Interv Radiol* 19:393–399
- Herrmann J, Krstin N, Schoennagel BP et al (2012) Age-related distribution of vertebral bone-marrow diffusivity. *Eur J Radiol* 81:4046–4049
- Savvopoulou V, Maris TG, Vlahos L, Mouloupoulos LA (2008) Differences in perfusion parameters between upper and lower lumbar vertebral segments with dynamic contrast-enhanced MRI (DCE MRI). *Eur Radiol* 18:1876–1883
- Nakanishi K, Gutzeit A (2010) Evaluation of malignant bone disease using DW-MRI. In: Koh DM, Thoeny HC (eds) *Diffusion-weighted MR imaging applications in the body*. Springer, Heidelberg, pp 207–226
- Vande Berg BC, Malghem J, Lecouvet FE, Maldague B (1998) Magnetic resonance imaging of the normal bone marrow. *Skelet Radiol* 27:471–483
- Lecouvet FE, Larbi A, Pasoglou V et al (2013) MRI for response assessment in metastatic bone disease. *Eur Radiol* 23:1986–1997
- Nonomura Y, Yasumoto M, Yoshimura R et al (2001) Relationship between bone marrow cellularity and apparent diffusion coefficient. *J Magn Reson Imaging* 13:757–760
- Padhani AR, Gogbashian A (2011) Bony metastases: assessing response to therapy with whole-body diffusion MRI. *Cancer Imaging* 11 Spec No A:S129–S145